Available online at www.sciencedirect.com
ScienceDirect
Trans. Nonferrous Met. Soc. China 28(2018) 1311−1320
Transactions of Nonferrous Metals Society of China
www.tnmsc.cn

Evolution and distribution of Al_2Sm phase in as-extruded AZ61−xSm magnesium alloys during semi-solid isothermal heat-treatment

Chen-liang CHU[1], Zhi HU[1,2], Xiao LI[1], Hong YAN[1,2], Xiao-quan WU[1], Yuan-lu MAI[1]

1. Institute of Advanced Forming, Nanchang University, Nanchang 330031, China;
2. Key Laboratory of Light Alloy Preparation & Processing in Nanchang City, Nanchang University, Nanchang 330031, China

Received 26 April 2017; accepted 10 November 2017

Abstract: The evolution and distribution of Al_2Sm phase in as-extruded AZ61−xSm (x=0, 1.5, 2.0 and 2.5, mass fraction, %) magnesium alloys during semi-solid isothermal heat treatment were investigated. The results showed that when as-extruded AZ61 magnesium alloys were modified with Sm, the smaller and rounder grains were obtained during semi-solid isothermal heat treatment. When the Sm content is 2.0% (mass fraction), the average size of the globular grains reached the smallest value of 90 μm. Although a few Al_2Sm particles existed in the α-Mg grains, most of Al_2Sm particles solidified at the edge of the globular grains with the width of ~20 μm. These phenomena are mainly attributed to the forces acting on Al_2Sm particles in front of the solid−liquid interface, leading to Al_2Sm particles accumulating at the solid−liquid interface and then solidifying at the edge of the globular grains in the quenching process.

Key words: magnesium alloy; rare earth element; semi-solid isothermal heat treatment; Al_2Sm particle

1 Introduction

As one of the lowest density structural materials, magnesium alloy has the advantages of high specific stiffness, high specific strength, good electrical conductivity, easy mechanical processing and recycling, allowing it to be one of the "Environment Friendly Materials in Present and Future Generations" [1]. In recent years, rare earth elements have been added into the magnesium alloys to improve their poor creep resistance, corrosion resistance, and their lack of fluidity in the casting process, leading to the development of various advanced magnesium alloy materials, such as WE54 and AE44 [2−4]. However, magnesium alloy has a hexagonal close-packed (hcp) crystalline structure; this particular structure only has three slip systems, which negatively impacts the plastic forming abilities of magnesium alloy.

In addition to offering significantly reduced forming loads, thixoforming technology also provides the opportunity to improve the plastic deformation ability of the alloys, as well as the ability to produce complex geometry components; such advantage provides a way to solve the problems of traditional plastic forming of wrought magnesium alloys, such as AZ31 and AZ61 [5−7]. In general, thixoforming technology is primarily composed of semi-solid material production, partial remelting, and thixoforming, with the semi-solid material production holding the most importance. Recent reports suggest that semi-solid isothermal heat treatment fulfills the semi-solid non-dendritic microstructure during heating prior to thixoforming and could omit the special procedure needed to fabricate the semi-solid materials [8,9]. Therefore, semi-solid rare earth−magnesium alloys prepared by semi-solid isothermal heat treatment have been investigated. HU et al [10] reported the rare earth metal Ce can hinder aggregation and association of the primary solid particles, inhibit solid particle growth, and form fine well-distributed round semi-solid microstructures. In addition, NAMI et al [11] revealed that the coarsening kinetics of the solid globular particles in a semi-solid slurry of AZ91 alloy satisfied the Ostwald ripening theory. It was shown

Foundation item: Project (51405216) supported by the National Natural Science Foundation of China; Project (20153BCB23023) supported by the Training Programme Foundation for Young Scientists of Jiangxi Province, China
Corresponding author: Zhi HU; Tel: +86-791-83969633; E-mail: huzhi@ncu.edu.cn
DOI: 10.1016/S1003-6326(18)64768-5

that by adding RE elements into AZ91 alloy, especially at 580 °C, the coarsening rate of the solid particles decreased, which resulted in smaller particle sizes. During semi-solid isothermal heat treatment, Mg atoms in the alloys would be rearranged and form solid globular particles. However, the discussion about evolution and distribution of RE-rich intermetallic compounds during the rearrangement of Mg atoms is very limited.

In recent years, the microalloying effects of the Mg−Al series magnesium alloys with the addition of Sm had been widely reported [12−14]. The Al_2Sm intermetallic compounds that were formed in the Mg−Al series magnesium alloys could cause heterogeneous nucleation, effectively prohibit dislocation movement and grain boundary sliding, and reduce the corrosion potential between the β-$Mg_{17}Al_{12}$ and α-Mg, thereby improving the mechanical properties and corrosion resistance of the alloys [15,16]. However, there still lacks enough experimental evidences to prove that rare earth atoms and their intermetallic compounds would enrich at solid−liquid interface during solidification. The microstructure of semi-solid metals both has solid and liquid phase and could be maintained by quenching process, which provides a new method to observe the distribution of RE-rich phase in the alloys. Therefore, the microstructure evolution of hot-extruded AZ61 wrought magnesium alloys with the addition of Sm during semi-solid isothermal heat treatment is investigated in this work, focusing specifically on the evolution and distribution of the Al_2Sm phase during semi-solid isothermal heat treatment.

2 Experimental

The chemical composition of AZ61−*x*Sm (*x*=0, 1.5, 2.0 and 2.5, mass fraction, %) magnesium alloy is shown in Table 1. Four alloy samples with a uniform, basic composition of AZ61 magnesium alloy were melted at 750 °C in a steel crucible inside a resistant furnace for 20 min with an SF_6 and CO_2 atmosphere. Three of the melts were added with 1.5%, 2.0%, and 2.5% Sm (in the form of Mg−15%Sm master alloy), respectively; they were then treated by high-energy ultrasound vibration for 2 min at 750 °C. The power of the ultrasonic generator was 0.6 kW and the frequency was 20 kHz. The fourth alloy (without Sm) served as the control, and was prepared under the same condition throughout the entire experiment. At 700 °C, the melts were poured into metallic molds with dimensions of 150 mm in length and 40 mm in diameter. The AZ61 alloys were homogenized at 400 °C for 10 h, and then hot-extruded after holding for 1 h at 400 °C. The extrusion ratio and the extrusion rate of the extruded bars were 6.25 and 2.5 m/min, respectively. The samples with the dimensions of 10 mm in length and 16 mm in diameter were processed from extruded bars for semi-solid isothermal heat treatment.

Table 1 Chemical compositions of AZ61−*x*Sm magnesium alloys (mass fraction, %)

Alloy	Al	Zn	Mn	Sm	Mg
AZ61	5.54	1.00	0.33	−	Bal.
AZ61−1.5Sm	5.45	0.95	0.30	1.71	Bal.
AZ61−2.0Sm	5.59	1.07	0.32	2.13	Bal.
AZ61−2.5Sm	5.61	1.09	0.30	2.51	Bal.

The semi-solid isothermal heat treatment was performed in an electric resistant furnace under an SF_6 and CO_2 atmosphere. When the furnace was heated to 570, 580, 590 and 600 °C, the different composition samples were put into the furnace and held for 0, 10, 15, 20 and 25 min, respectively. After the isothermal heat treatment, the samples were immediately quenched in cold water.

The samples were prepared with standard metallographic procedures. An etchant of 4% nitric acid in an alcohol solution was used to reveal the microstructures of the polished specimens. Another 1 mm-thick slice sample for TEM was perpendicularly cut from hot-extruded AZ61−2.0Sm magnesium alloy treated by isothermal heat treatment. The sample were ground and polished on both sides to about 70 μm thick. Then, ion beam thinning was carried out to ensure that the thickness of the sample achieved the requirement of TEM. Microstructure characterization was carried out with optical microscopy (Nican M200). Precipitated phases in the AZ61−*x*Sm magnesium alloys were characterized by scanning electron microscopy (SEM, FEI Quanta 200F), energy dispersive spectroscopy (EDS), and transmission electron microscope (TEM, JEM−2100).

3 Results

3.1 Microstructural characterization

Figure 1 displays the SEM images and EDS analysis results of the AZ61−2.0Sm magnesium alloy. It could be seen in hot-extruded state (Fig. 1(a)) that all the white phases distributed along the extrusion direction. According to the EDS analysis result of Point 1, the white phase was a type of Sm-rich phase. When the hot-extruded AZ61−2.0Sm magnesium alloys were treated by semi-solid isothermal heat treatment at 580 °C for 10 and 15 min, the microstructure of the alloys changed into fine, nearly spherical grains with the average size of 90 μm. Some small liquid pools formed within the spherical grains, as shown in Fig. 1(b) (marked as Point 2). Moreover, instead of distributing only along the extrusion direction, white Sm-rich phases

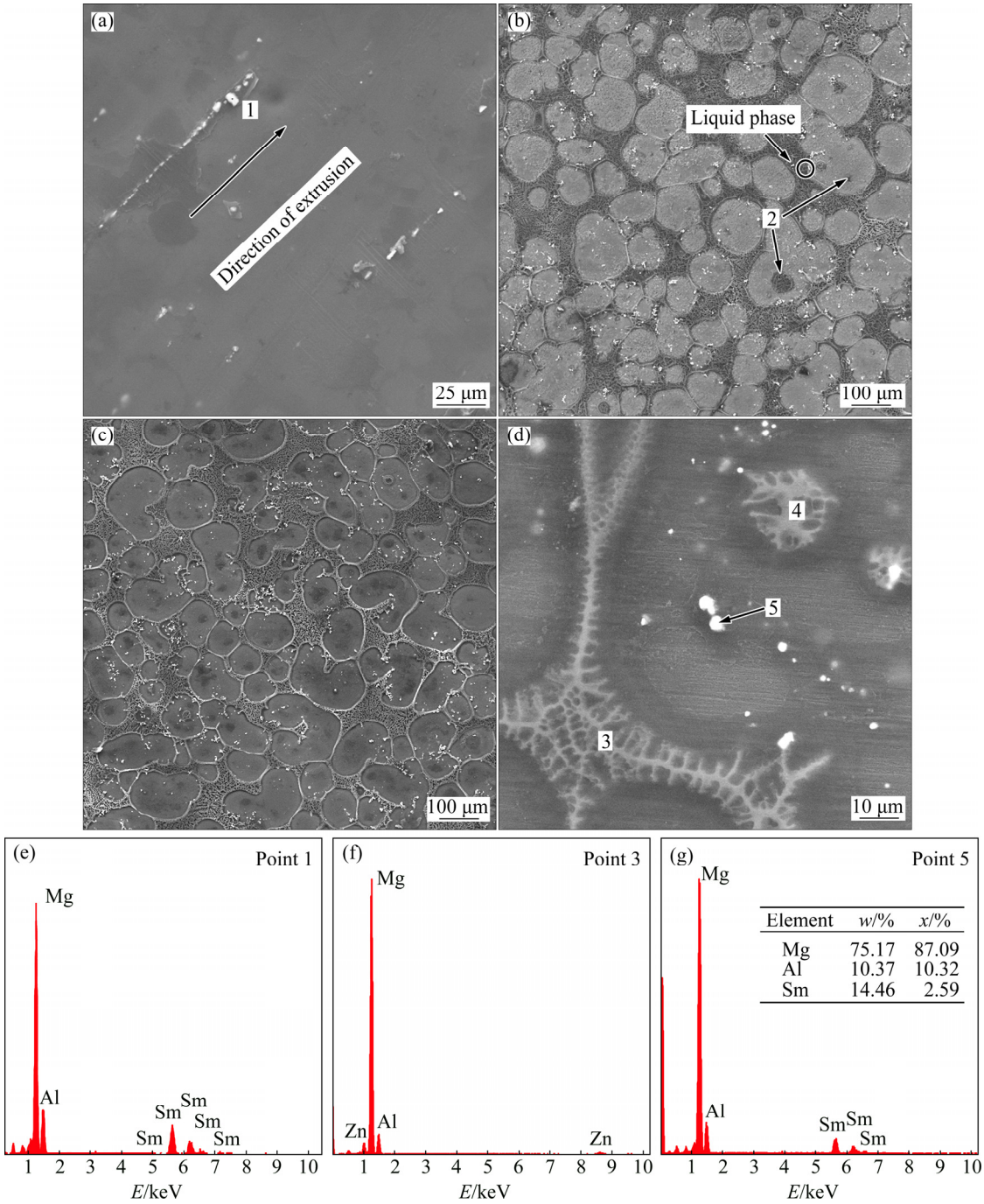

Fig. 1 SEM images (a−d) and EDS analysis result (e−g) of AZ61−2.0Sm magnesium alloy: (a) Hot-extruded; (b) Treated by isothermal heat treatment at 580 °C for 10 min; (c) Treated by isothermal heat treatment at 580 °C for 15 min; (d) More detail of liquid phase in (b); (e) EDS of Point 1; (f) EDS of Point 3; (g) EDS of Point 5

uniformly distributed throughout the treated alloy. Although some Sm-rich phases formed within the spherical grains, more Sm-rich phases enriched at the edge of spherical grains. The liquid phase in the treated alloy was observed by further amplification, as shown in Fig. 1(d). When the semi-solid microstructures were quenched, the liquid phases (marked as Point 3) and small liquid pools (marked as Point 4) in the treated alloy were rapidly cooled, and a number of fine primary dendrites and secondary dendrites formed in the liquid phase. The main components of these dendrites are Mg, Al and Zn, as shown in Fig. 1(f). It was worth noting that many white particles with the size of ~4 μm (marked as Point 5) had a similar chemical composition with Point 1, and predominantly distributed in the annular region with the width of ~20 μm between the liquid phase and the central areas of spherical grains, as shown in Figs. 1(d) and (g). Therefore, it could be inferred that a large

number of Sm-rich phases, enriching at solid−liquid interface, quickly solidified at the edge of the spherical grains under the condition of quenching.

The surface mapping images of Sm-rich phases are shown in Fig. 2. It was worth noting that many Al elements distributed in the liquid phase and small liquid pool in the α-Mg grains. Moreover, the main components of the white particles around the α-Mg grains in the alloy were Al and Sm elements. Figure 3 shows TEM images of the hot-extruded AZ61−2.0Sm magnesium alloy. As

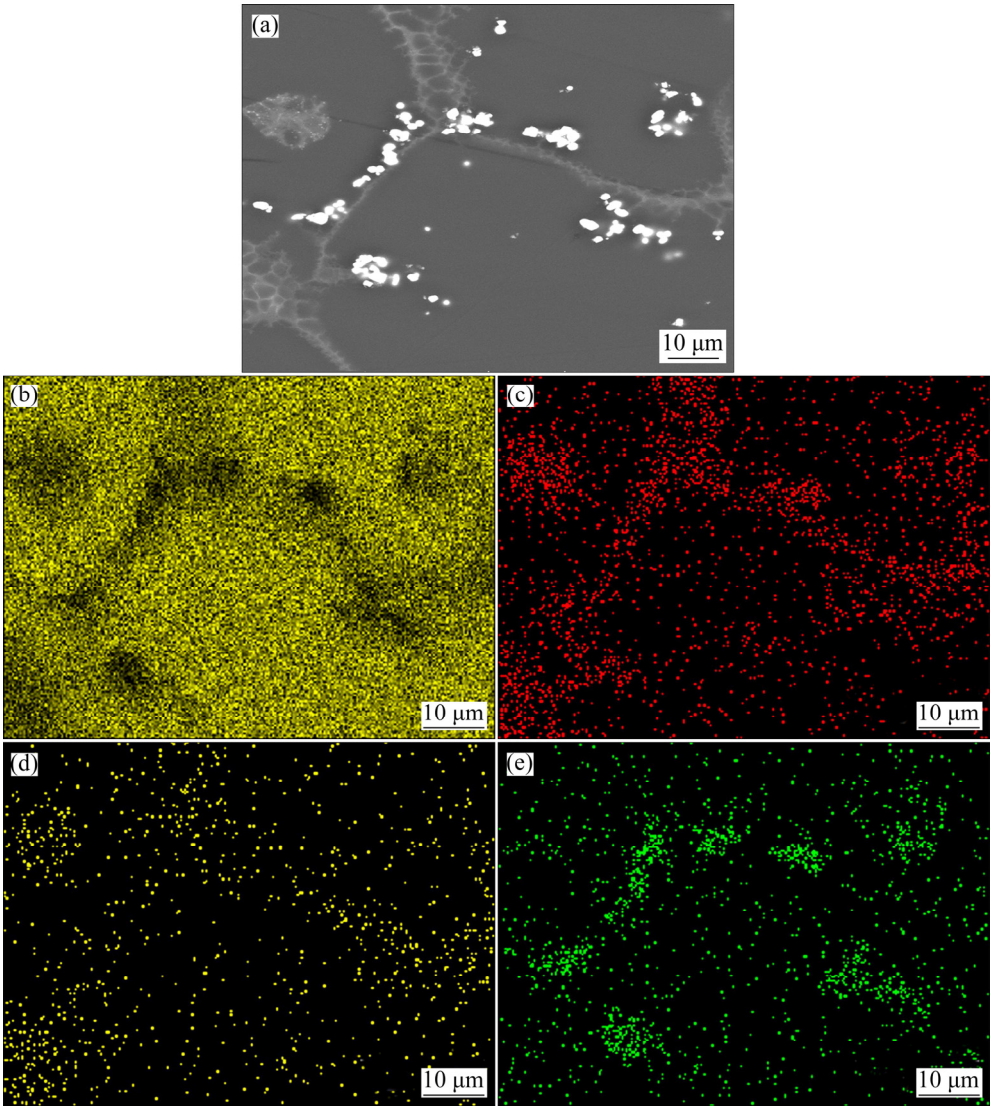

Fig. 2 Surface scanning images of Sm-rich phases in AZ61−2.0Sm alloy: (a) SEM micrograph; (b) Mg; (c) Al; (d) Zn; (e) Sm

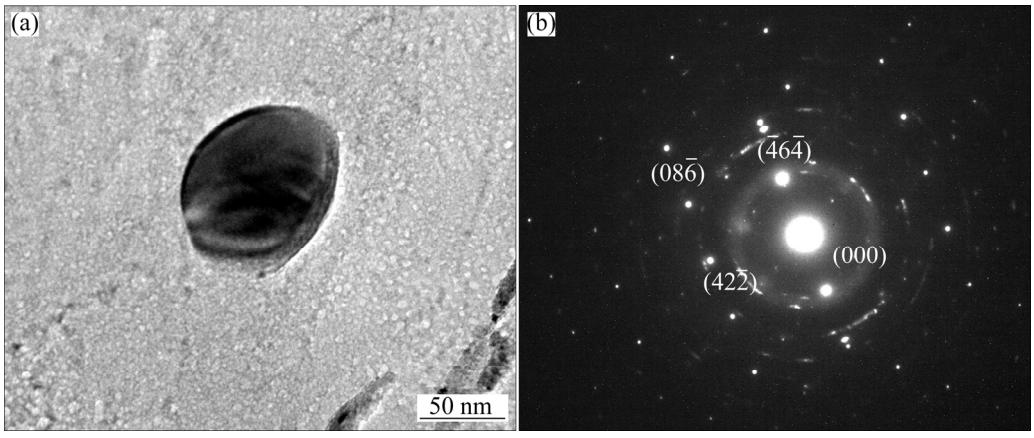

Fig. 3 TEM images of AZ61−2.0Sm magnesium alloy treated by isothermal heat treatment: (a) Al_2Sm phase; (b) Diffraction pattern

shown in Figs. 3(a) and (b), the black Sm-rich phase with the size of 80 nm inside the alloy was characterized by selected area diffraction patterns. The result showed that the face centered cubic structure of Sm-rich particles was Al_2Sm phases.

3.2 Semi-solid microstructural evolution

Figure 4 shows the semi-solid microstructure of AZ61−2.0Sm magnesium alloy treated at various heat treatment temperatures for 10 min. As shown in Fig. 4(a), when the alloys were treated by a semi-solid isothermal heat treatment at 570 °C, morphology of the α-Mg grain in the alloy presented polygon-like shape with some sharp corners. Some grains and grain boundaries were melted into the liquid phase. These liquid phases distributed in the grain boundary and the interior of the α-Mg grains. With the increase of the isothermal temperature (Fig. 4(b)), the α-Mg grains became uniform and spheroidized with a much smaller size. When the isothermal temperature reached 590 °C (Fig. 4(c)), the microstructure of the alloys modified with 2.0% Sm finally became more refined and more spherical in shape. The content of liquid phase was far more than that of the alloys treated at 570 and 580 °C. When the isothermal heat treatment temperature reached 600 °C, the spherical effect of the grains decreased and dendrite-like grains appeared, as shown in Fig. 4(d).

Figure 5 shows the semi-solid microstructure of the AZ61−2.0Sm magnesium alloy treated at 580 °C for various time from 0 to 25 min. As shown in Fig. 5(a), a large number of primary polygonal α-Mg grains formed in the alloy after being held for 0 min. After 10 min holding (Fig. 5(b)), the liquid phase appeared both in grain boundary and inside the grain. Meanwhile, the α-Mg grains became increasingly smaller and rounder in shape. When the holding time was prolonged to 15 min, the α-Mg grains in the alloy also displayed round and refined features, as shown in Fig. 5(c). Further extending the holding time to 20 min led to the coarsening of the α-Mg particles and the formation of the irregularly polygonal α-Mg particles (Fig. 5(d)). When the holding time reached 25 min, it could be seen from Fig. 5(e) that many fine α-Mg grains distributed around of the coarse α-Mg grains in the alloy. The reason for this phenomenon can be described by Ostwald ripening mechanism, which operates through the dissolution of small particles and the growth of large particles. Moreover, the Ostwald ripening mechanism can be described by the classical LSW relationship [17]:

$$d_t^3 = d_0^3 + kt \tag{1}$$

where d_0 is the initial particle size, d_t is the size at time t and k is the coarsening rate constant. It is apparent that the α-Mg particles grow as the holding time is prolonged.

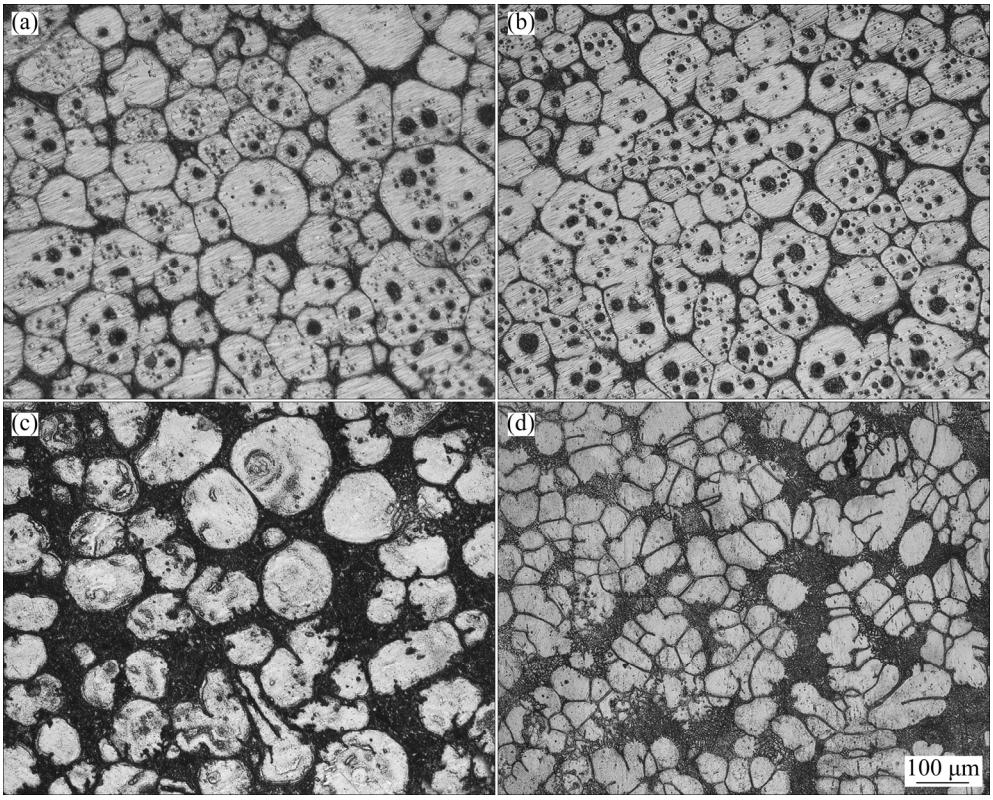

Fig. 4 Microstructures of AZ61−2.0Sm magnesium alloy treated at various isothermal temperatures for 10 min: (a) 570 °C; (b) 580 °C; (c) 590 °C; (d) 600 °C

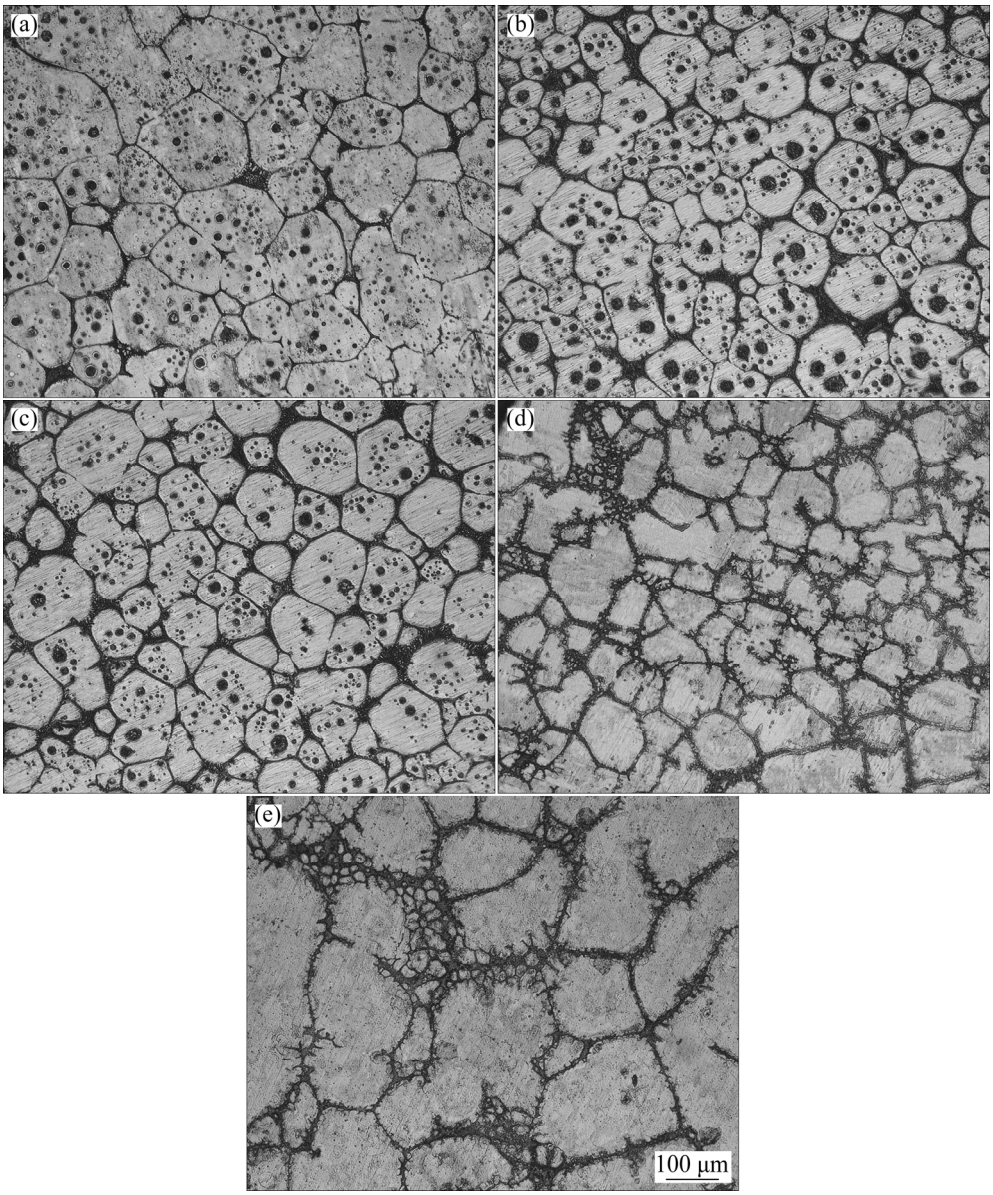

Fig. 5 Semi-solid microstructures of AZ61−2.0Sm magnesium alloy treated at 580 °C for different holding time: (a) 0 min; (b) 10 min; (c) 15 min; (d) 20 min; (e) 25 min

Figure 6 shows the semi-solid microstructures of the AZ61−*x*Sm magnesium alloy at 580 °C for 10 min. It could be seen that the microstructure of the *α*-Mg particles changed from polygonal-like to globular-like with the increase of Sm content. When 2.0% Sm was added to the alloy, the smallest and roundest grains were obtained, as shown in Fig. 6(c). The average grain diameter and aspect ratio were used to evaluate the effect of Sm content on the microstructure of as-extruded AZ61 magnesium alloys, with the results exhibited in Fig. 7. The average grain diameter and aspect ratio of the matrix were 185 μm and 1.47, respectively. With the increase of Sm content, the value of the average grain diameter and aspect ratio of the alloys both decreased and achieved the lowest value when the Sm content is 2.0% and were about 90 μm and 1.13, respectively. However, when Sm exceeded a certain content, Al_2Sm phases would partially gather and their size became larger. The segregation of Al_2Sm phase at the solid−liquid interface made the degree of undercooling decrease, causing the *α*-Mg grain to grow.

4 Discussion

During semi-solid isothermal heat treatment, the Mg atoms in the alloys were rearranged, leading to the microstructure of the as-extruded magnesium alloys changing from vimineous or fine, equiaxed grains to semi-solid globular ones. In this work, the effects of the second phase Al_2Sm particles on the microstructure of

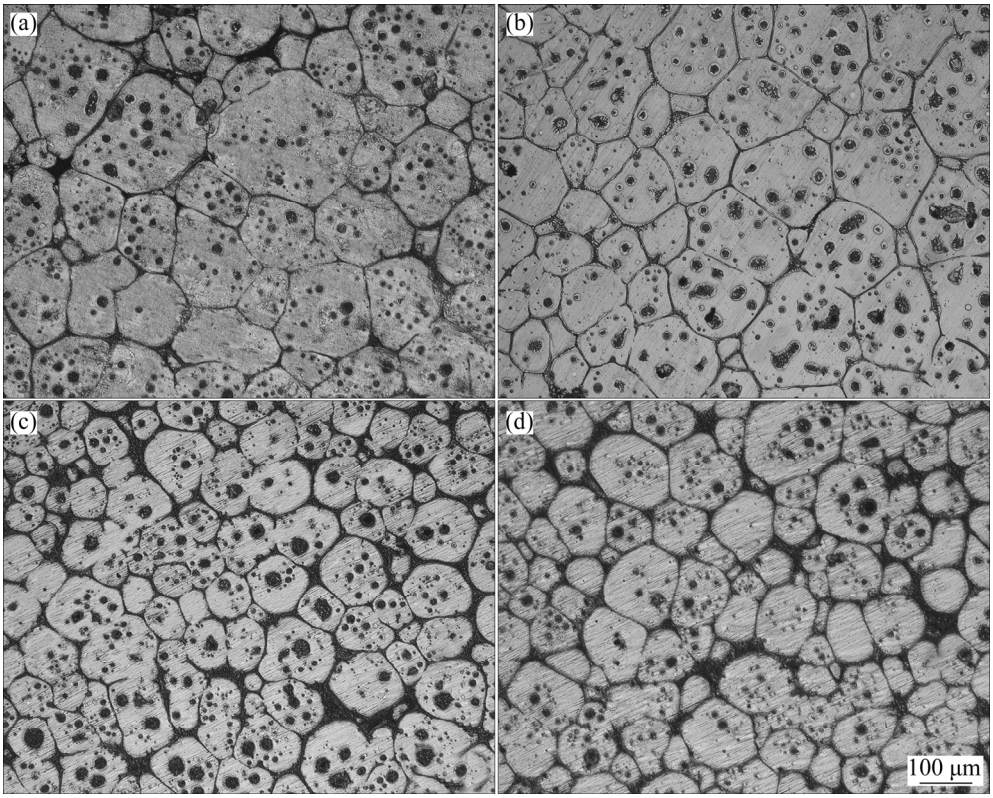

Fig. 6 Semi-solid microstructures of AZ61−*x*Sm magnesium alloys with different Sm contents isothermally-treated at 580 °C for 10 min: (a) 0%; (b) 1.5%; (c) 2.0%; (d) 2.5%

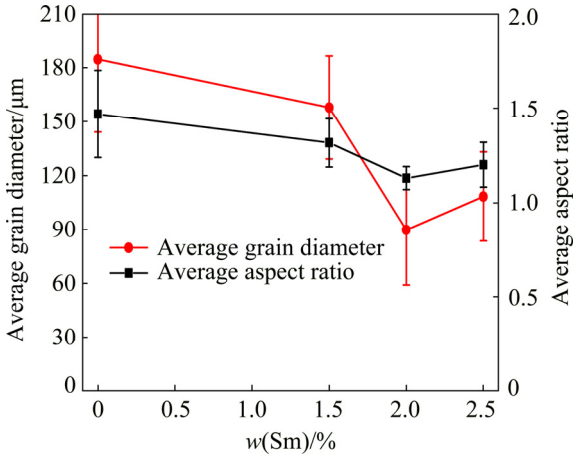

Fig. 7 Average grain diameter and aspect ratio with change of Sm content of AZ61−*x*Sm alloys isothermally-treated at 580 °C for 10 min

the alloys were discussed, and a schematic diagram of the Al_2Sm phase evolution in hot-extruded AZ61−*x*Sm magnesium alloys during semi-solid isothermal heat treatment is presented in Fig. 8.

The initial extruded grain morphology is composed of the vimineous α-Mg grains and the second phase Al_2Sm. As shown in Fig. 8(a) and Fig. 1(a), the fine Al_2Sm particles mainly distributed within grain boundaries along the extrusion direction. When the samples were treated with semi-solid isothermal heat treatment, the vimineous grains in the alloy began to melt and fractured into fine polygon particles. As shown in Fig. 8(b) and Fig. 1(b), a small number of Al_2Sm particles existed in the α-Mg grains. However, most of Al_2Sm particles distributed at the front edge of the liquid and the interface of the α-Mg grains. As illustrated in Fig. 9, the reason for this is that several forces act upon the Al_2Sm particle ahead of an advancing solid−liquid interface during solidification of the liquid containing Al_2Sm particles. The primary forces are the viscous drag force F_D, the interfacial force F_I, and F_σ, the force attributed to the interfacial energy gradient on the particle. F_D, F_I and F_σ for a spherical particle ahead of a nonplanar interface can be expressed as [18]

$$F_D = 6\pi\eta V_S \frac{R^2}{h}\alpha^2 \tag{2}$$

$$F_I = 2\pi R\Delta\gamma\alpha \tag{3}$$

$$F_\sigma = -\frac{8}{3}\pi R^2 K \tag{4}$$

$$\alpha = \frac{R_I}{R_I - R} \tag{5}$$

where R is the particle radius, η is the liquid viscosity, V_S is the interface velocity, h is the particle−interface distance, α is the interface shape factor, R_I is the interface radius, $\Delta\gamma$ is the variation of interfacial energy with

particle−interface distance h, and K is the interfacial energy gradient. The force F_σ is usually attractive, pushing particles from liquids to solids. The larger the interfacial energy gradient K is, the larger the force F_σ is. Therefore, Al_2Sm particles are eventually pushed ahead of the liquid phase. The viscous drag force F_D is always attractive, favoring particle engulfment; on the other hand, the interfacial force F_I is usually repulsive, favoring particle pushing. When the three forces reach a balanced state $F_D+F_\sigma=F_I$, Al_2Sm particles preferentially accumulate at the solid−liquid interface, as shown in Fig. 1(b) and Fig. 8(b). A similar phenomenon of alumina inclusions during solidification has been reported [19].

Moreover, many high density dislocations form after severe plastic deformation and usually accumulated around the grain boundaries, leading to blocked dislocation motions [20]. At the same time, the amplitude of atomic vibration is intensified with the increase of temperature. The pile-up of dislocations makes the deformed grains urge to seek the recrystallization core near the grain boundary [21]. Therefore, the Al_2Sm particles distribute at the front edge of the liquid and α-Mg grain interfaces are beneficial to the formation of recrystallization grains. According to Ref. [22], the Al_2Sm phases with a higher melt point (T_m=1480 °C) and good thermal stability have a low planar disregistry value of 0.45% with α-Mg phase, which is far less than the most effective nucleation value of 6%. Therefore, part of Al_2Sm particles act as a heterogeneous nucleation core in the α-Mg phase, promoting the formation of grain recrystallization in the alloys.

As shown in Fig. 6(c), vimineous grains in the alloys are replaced by fine, globular semi-solid particles with the increase of the treating temperature and holding time. The Al_2Sm particles still accumulate at the solid−liquid interface, which leads to the degree of undercooling greatly increasing and promotes the formation of nucleus. Meanwhile, the Al_2Sm phases distributing among α-Mg grains can also mechanically hinder the growth of α-Mg grains [23]. When the content of Al_2Sm phase is enough for the heterogeneous nucleation in the alloy, the residual Al_2Sm particles would impede the flow of liquid between grain and boundary in the mutual fusion process, finally forming small liquid pools in the grain. With the increase in holding time, Ostwald ripening occupies a dominant position and competitive grain growth takes the leading role, resulting in small grains melting or being swallowed by larger grains.

When the samples were treated by the quenching process in cold water, the semi-solid microstructure of

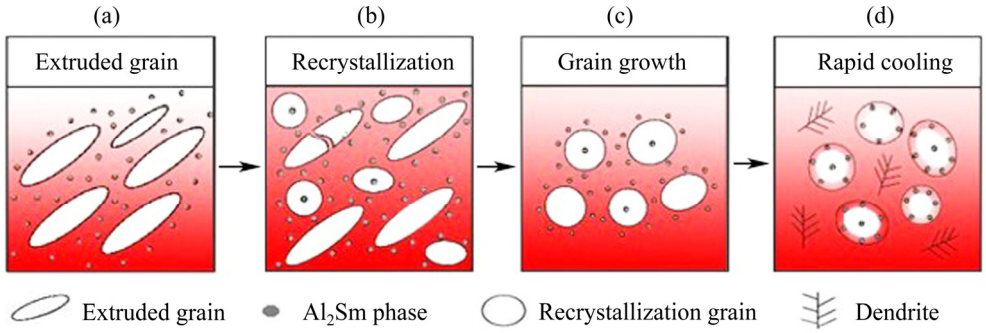

Fig. 8 Schematic diagram of Al_2Sm phase evolution in hot-extruded AZ61−xSm magnesium alloys during semi-solid isothermal heat treatment

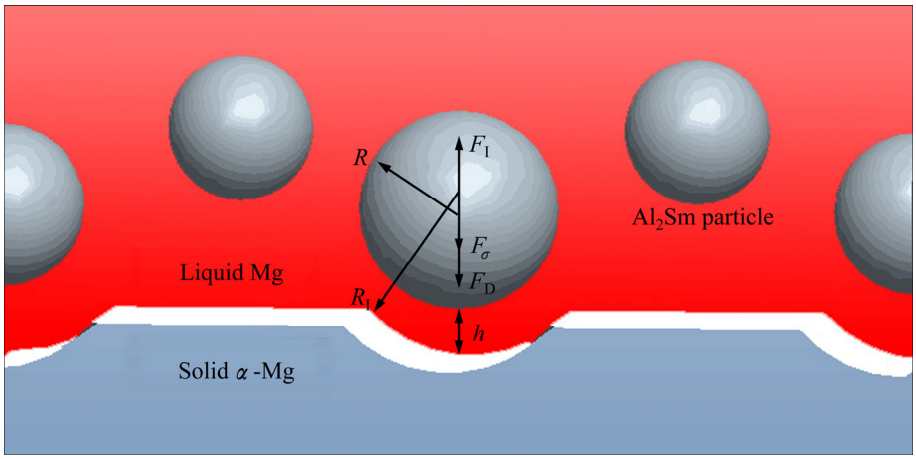

Fig. 9 Forces acting on Al_2Sm particle in front of solid−liquid interface

the samples was maintained, as shown in Fig. 8(d). A large number of fine primary dendrites and secondary dendrites formed during the quenching process of the liquid in the semi-solid samples. Meanwhile, many Al_2Sm particles solidified between the liquid phase and the solid α-Mg grains. An annular solidified region with the width of ~20 μm formed during quenching process, as shown in Figs. 8(d) and 1(b) and 1(d). Therefore, it can be inferred that the particle−interface distance h in Eq. (2) is less than 20 μm. Moreover, due to the Al_2Sm particles being pushed ahead of the liquid phase according to Eq. (4), no Al_2Sm particles were observed within the liquid or the α-Mg dendrites of the alloys.

5 Conclusions

1) The microstructure of the as-extruded AZ61−xSm magnesium alloys treated by semi-solid isothermal heat treatment present fine and nearly spherical grains. Many Al_2Sm intermetallic compounds with size of ~4 μm solidified at the edge of the globular grains with a width of ~20 μm. This phenomenon is ascribed mainly to forces acting on Al_2Sm particles in front of the solid−liquid interface, leading to Al_2Sm particles accumulating at the solid−liquid interface and then solidifying at the edge of the globular grains in the quenching process.

2) Smaller and rounder grains formed within the Sm-modified alloys during semi-solid isothermal heat treatment. When the Sm content is 2.0% (mass fraction), the average size of the globular grains reached the smallest value of 90 μm. With the increase of treating temperature and holding time, the globular grains tended to coarsen as a result of Ostwald ripening.

References

[1] MEENASHISUNDARAM G K, GUPTA M. Emerging environment friendly, magnesium-based composite technology for present and future generations [J]. the Journal of the Minerals, Metals & Materials Society, 2016, 68: 1890−1901.

[2] ZHANG Wen-qiang, XIAO Wen-long, WANG Fang, MA Chao-li. Development of heat resistant Mg−Zn−Al-based magnesium alloys by addition of La and Ca: Microstructure and tensile properties [J]. Journal of Alloys and Compounds, 2016, 684: 8−14.

[3] YANG Qiang, GUAN Kai, BU Fang-qiang, ZHANG Ya-qin, QIU Xin, ZHENG tian, LIU Xiao-juan, MENG Jian. Microstructures and tensile properties of a high-strength die-cast Mg−4Al−2RE−2Ca−0.3Mn alloy [J]. Materials Characterization, 2016, 113: 180−188.

[4] LIU Ning-yuan, ZHANG Zhen-yan, PENG Li-ming, DING Wen-jiang. Microstructure evolution and mechanical properties of Mg−Gd−Sm−Zr alloys [J]. Materials Science and Engineering A, 2015, 627: 223−229.

[5] SALLEH M S, OMAR M Z, ALHAWARI K S, MOHAMMED M N, MAD ALI M A, MOHAMAD E. Microstructural evolution and mechanical properties of thixoformed A319 alloys containing variable amounts of magnesium [J]. Transactions of Nonferrous Metals Society of China, 2016, 26: 2029−2042.

[6] SHABESTARI S G, SAGHAFIAN H, SAHIHI F, GHONCHEH M H. Investigation on microstructure of Al−25wt%Mg_2Si composite produced by slope casting and semi-solid forming [J]. International Journal of Cast Metals Research, 2015, 28: 158−166.

[7] CHEN Tian, XIE Zhi-wen, LUO Zhuang-zhu, YANG Qin, TAN Sheng, WANG Yun-jiao, LUO Yi-min. Microstructure evolution and tensile mechanical properties of thixoformed AZ61 magnesium alloy prepared by squeeze casting [J]. Transactions of Nonferrous Metals Society of China, 2014, 24: 3421−3428.

[8] YANG Ming-bo, PAN Fu-sheng, CHENG Ren-ju, BAI Liang. Effect of semi-solid isothermal heat treatment on the microstructure of Mg−6A1−1Zn−0.7Si alloy [J]. Journal of Materials Processing Technology, 2008, 206: 374−381.

[9] MA G R, LI X L, XIAO L, LI Q F. Effect of holding temperature on microstructure of an AS91 alloy during semisolid isothermal heat treatment [J]. Journal of Alloys and Compounds, 2010, 496: 577−581.

[10] HU Yong, LI Rao, LI Qing-ping, WAN Qiang. Effect of isothermal heat treatment on the microstructure of semi-solid AZ91D+Ce magnesium alloy [J]. Rare Metal Materials and Engineering, 2016, 45: 493−497.

[11] NAMI B, SHABESTARI S G, MIRESMAEILI S M, RAZAVI H, MIRDAMADI S. The effect of rare earth elements on the kinetics of the isothermal coarsening of the globular solid phase in semisolid AZ91 alloy produced via SIMA process [J]. Journal of Alloys and Compounds, 2010, 489: 570−575.

[12] WANG Cun-long, DAI Ji-chun, LIU Wen-cai, ZHANG Liang, WU Guo-hua. Effect of Al additions on grain refinement and mechanical properties of Mg−Sm alloys [J]. Journal of Alloys and Compounds, 2015, 620: 172−179.

[13] WU Dao-gao, YAN Shi-hong, WANG Zhi-qiang, ZHANG Zhi-qi, MIAO Rui-ying, ZHANG Xiao-wei, CHEN De-hong. Effect of samarium on microstructure and corrosion resistance of aged as-cast AZ92 magnesium alloy [J]. Journal of Rare Earths, 2014, 32: 663−671.

[14] LUO Xiao-ping, FANG Da-qing, LI Qiu-shu, CHAI Yue-sheng. Microstructure and mechanical properties of an Mg−4.0Sm−1.0Ca alloy during thermomechanical treatment [J]. Journal of Rare Earths, 2016, 34: 1134−1138.

[15] HU Zhi, LI Xiao, HUA Qun, YAN Hong, QIU Hong-xu, RUAN Xian-ming, LI Zheng-hua. Effects of Sm on microstructure and corrosion resistance of hot-extruded AZ61 magnesium alloys [J]. Journal of Materials Research, 2015, 30: 3671−3681.

[16] HU Zhi, LI Xiao, YAN Hong, WU Xiao-quan, HUA Qun, LIN Jing-wu. Effects of ultrasonic vibration on microstructure evolution and elevated-temperature mechanical properties of hot-extruded Mg−6Al−0.8Zn−2.0Sm wrought magnesium alloys [J]. Journal of Alloys and Compounds, 2016, 685: 58−64.

[17] ZHU Guang-lei, XU Jun, ZHANG Zhi-feng, LIU Guo-jun. Effect of high shear rate on solidification microstructure of semisolid AZ91D alloy [J]. Transactions of Nonferrous Metals Society of China, 2010, 20: 868−872.

[18] SHANGGUAN D, AHUJA S, STEFANESCU D M. An analytical model for the interaction between an insoluble particle and an advancing solid liquid interface [J]. Metallurgical and Materials Transactions A, 1992, 23: 669−680.

[19] ZHENG Li-chun, MALFLIET A, WOLLANTS P, BLANPAIN B, GUO Mu-xing. Effect of surfactant Te on the behavior of alumina inclusions at advancing solid−liquid interfaces of liquid steel [J]. Acta Materialia, 2016, 120: 443−452.

[20] GUO Fei, ZHANG Ding-fei, WU Hua-yi, JIANG Lu-yao, PAN Fu-sheng. The role of Al content on deformation behavior and related texture evolution during hot rolling of Mg−Al−Zn alloys [J]. Journal

of Alloys and Compounds, 2017, 695: 396−403.
[21] FATEMI S M, ZAREI-HANZAKI A, PAUL H. Strain-induced nano recrystallization in AZ31 magnesium: TEM characterization [J]. Journal of Alloys and Compounds, 2017, 699: 796−802.
[22] HU Xiao-yu, FU Peng-huai, DAVID S, PENG Li-ming, SUN Ming, ZHANG Ming-xing. On grain coarsening and refining of the Mg−3Al alloy by Sm [J]. Journal of Alloys and Compounds, 2016, 663: 387−394.
[23] LI Ke-jie, LI Quan-an, JING Xiao-tian, CHEN Jun, ZHANG Xing-yuan, ZHANG Qing. Effects of Sm addition on microstructure and mechanical properties of Mg−6A−0.6Zn alloy [J]. Scripta Materialia, 2009, 60: 1101−1104.

挤压态 AZ61−*x*Sm 镁合金在半固态等温热处理中的 Al_2Sm 相演化和分布

褚晨亮[1]，胡 志[1,2]，李 晓[1]，闫 洪[1,2]，吴孝泉[1]，麦圆璐[1]

1. 南昌大学 先进成形研究所，南昌 330031；
2. 南昌大学 南昌市轻合金制备与加工重点实验室，南昌 330031

摘 要：研究挤压态 AZ61−*x*Sm(*x*=0, 1.5, 2.0, 2.5, 质量分数，%)镁合金在半固态等温热处理中的 Al_2Sm 相演化和分布规律。结果表明，含 Sm 的挤压态 AZ61 镁合金在半固态等温热处理中可以得到更细小、更圆整的晶粒。当 Sm 含量为 2.0%(质量分数)时，球状晶粒的平均尺寸达到最小值 90 μm。尽管部分 Al_2Sm 颗粒存在于 α-Mg 晶粒内部，但大多数 Al_2Sm 颗粒凝固于球状晶粒边缘~20 μm 处。导致这种现象的原因是：Al_2Sm 颗粒在固液前沿的受力状态导致其在固液界面处聚集并在随后的淬火过程中凝固在球状晶粒的边缘。

关键词：镁合金；稀土元素；半固态等温热处理；Al_2Sm 颗粒

(Edited by Bing YANG)